



OVERHEAD COOLING DEVICE REDUCING THERMAL STRATIFICATION AT DISPLACEMENT VENTILATION

Daniel Schmeling¹, Tobias Dehne¹, Pascal Lange¹, Axel Dannhauer¹, Andrei Shishkin¹ & Ingo Gores²

¹ German Aerospace Center (DLR), Institute of Aerodynamics and Flow Technology, Bunsenstr a e 10, 37073 G ttingen, Germany

² Airbus Operations GmbH, Kreetzlag 10, 21129 Hamburg, Germany

Abstract

We present a novel, patent-pending technology brick to reduce the thermal stratification under cabin displacement ventilation in a passenger aircraft. After the presentation of the new concept, we discuss different potential technical realizations of overhead cooling device. Finally, the positive effect of the new concept on the passenger comfort is evaluated by means of computational fluid dynamics analysis. Therefore, a generic long-range cabin with a nine-abreast seating is modelled for pure cabin displacement ventilation and with additionally activated cooling elements. The results proved, that the vertical temperature gradient is reduced and that a better predicted mean vote evaluation is achieved upon activation of the new elements.

Keywords: Passenger Aircraft Cabin; Displacement Ventilation; Thermal Comfort; "Radiant Cooling"; Operative Temperature

1. Introduction

For civil aviation, the environmental control systems (ECS) ensures a viable environment inside the passenger cabin in terms of pressure, temperature as well as oxygen supply and furthermore provides comfortable thermal conditions. Hereto, the heat that is released in the passenger compartment has to be removed by well-balanced and robust ventilation systems. As state-of-the-art, mixing ventilation, characterized by air supply below the ceiling and the lateral luggage bins is installed in all short- and long-range commercial passenger aircraft. Another ventilation concept that has not yet been used in aircraft cabins but has only been investigated in studies and described in patents, is based on floor-side displacement ventilation [1, 2]. Here, the air is supplied in the area of the floor with low momentum. Due to the heat loads in the aircraft cabin, in particular from the passengers, the fresh cabin air is heated locally, rises and finally leaves the cabin in the ceiling area.

The floor-side displacement ventilation has a weight savings potential compared to the mixing ventilation system due to the omission of e.g. rising ducts. Furthermore, displacement ventilation potentially results in a very high heat removal efficiency [2], which can be up to 0.9, while simultaneously providing low air velocities and a homogeneous spatial temperature distribution across the seats in the aircraft cabin. On the other side, disadvantages of floor-side displacement ventilation are strong vertical temperature stratification [3] and a rather high sensitivity on the supply air conditions with regard to the comfortable parameter. To overcome the drawback of potentially comfort-critical temperature stratifications, a technical solution is introduced, described and analysed in this work.

2. Proposed Solution

2.1 Concept

The patent-pending idea to reduce the temperature stratification of cabin displacement ventilation (CDV) is the integration of active cooling devices into the lower parts of the overhead luggage bins [4], see also Figure 1. The airflow itself will be similar as for plain CDV, whereas the “perceived” temperature especially in the head zone shall be decreased. To achieve a “radiant cooling” effect – being well aware, that this term is physically not correct – the surface of the overhead luggage bin needs to be cooled. Thereby, a well-balanced temperature control has to ensure, that the dew-point temperature is not undercut.

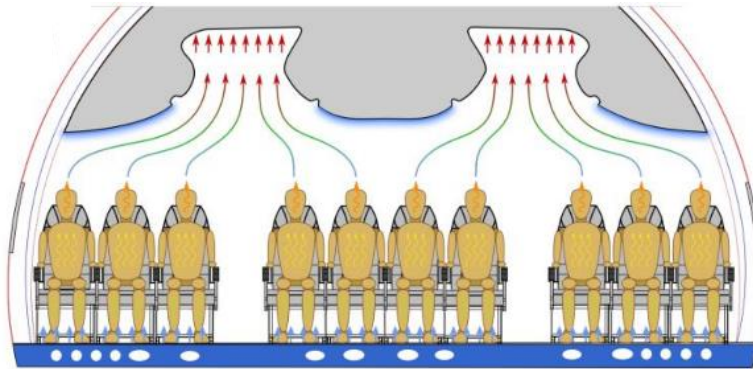


Figure 1: Integration of the cooling concept (light blue zones at the overhead compartments) at cabin displacement ventilation in the aircraft cabin.

2.2 Possible Technical Realizations

Three possible technical realisations are sketched in Figure 2: (a) with a heat exchanger element at the outer shell, (b) connected to the ECS system and (c) with a (thermo-electric) heat exchanger. Thereby, the first two concepts are shown with an active element (1) consisting of a porous material, whereas the third concept generates a well-guided air-jet along the surface of the element to reduce the surface temperature. It should be noted, that also other combinations of the sketched technical realisations are thinkable and included in the pending patent [4].

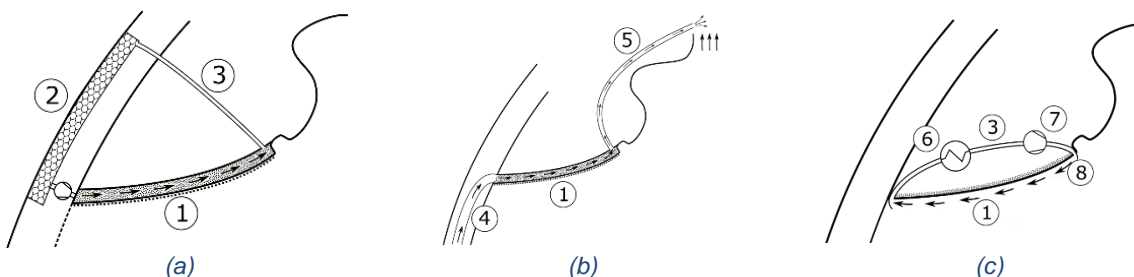


Figure 2: Possible technical realisations of the cooling element (a) as closed system with outer-shell heat exchanger, (b) as open system and (c) as closed system with (thermo-electric) heat exchanger. The number responds to (1) the active element, (2) a heat exchanger, (3) the recirc pipes, (4) a connection to the mixer unit, (5) an exhaust pipe, (6) a (thermo-electric) heat exchanger, (7) a controllable fan / pump and (8) a nozzle to generate an exhaust air jet following parallel to the active elements' surface. Following [4].

The first possible technical realization uses a heat exchanger at the outer shell (2) to reduce the temperature of the coolant to the desired value, see Figure 2 (a). A controllable pump or fan transports the coolant through the active element (1) and the recirc pipes (3). As a result, a closed system is realized, which only needs the electric supply for the pump. Main drawback of this system is that it will only work when the outer shell is cold, e.g. during cruise flight. For a hot-day-on-ground situation the additional cooling surface cannot be activated. However, the main advantage is that during cruise no additional energy for the operation of the active cooling elements is needed. The second concept (b) is depicted with a similar active element (1). The desired temperature reduction is achieved by a connection to the ECS system of the airplane (4). Using this connection, cold air from the ECS can

be guided through the active element and exhausted through an additional pipe (5). Main drawback of this concept is the required connection to the ECS, i.e. it cannot be installed as stand-alone system. On the other hand, the advantage is, that only small pipes to the ECS are needed, and no further e.g. electrical connections are needed. The last sketched possible technical realization (c) is again a stand-alone system similar to (a). The cooling demand will be provided e.g. by a thermo-electric heat exchanger (6) and a controllable fan (7). The latter provides the desired amount of air, which flows through the system. In contrast to both previous concepts, the active element itself is realized as an overflowed surface. A well-balanced system with a nozzle (8) and the shape of the element will ensure that the air follows the surface due to the Coandă effect. A possible drawback of this solution is the additional demand of electrical energy and the additional waste heat released by thermo-electric heat exchanger. Main advantage is, the capability for full integration in the overhead bin without any connections to the ECS or the outer shell.

All presented concepts and other combinations of them have their own advantages and disadvantages. Which solution is the most reasonable also depends on the application case. The previous discussion was rather aiming at highlighting that there are possible realizations and implementation approaches, than at presenting a final prototype.

3. Numerical Procedure

To validate the performance of the concepts with active cooling elements, numerical simulations are carried out using the high-performance computing (HPC) cluster of the Institute of Aerodynamics and Flow Technology in Göttingen. The commercial edition Engys of the open source computational fluid dynamics (CFD) toolkit OpenFOAM is used to perform the calculations and for the pre- and post-processing operations.

3.1 Computational Domain

The test configuration is a slightly simplified long-range cabin geometry with nine-abreast seating. The computational domain spans five rows with adiabatic, non-permeable boundary conditions in flight direction, see Figure 3 (a). A cross-section of the mesh with a sufficient grid refinement next to all surfaces, i.e. the surrounding boundaries and the thermal manikins, is sketched in Figure 3 (b).

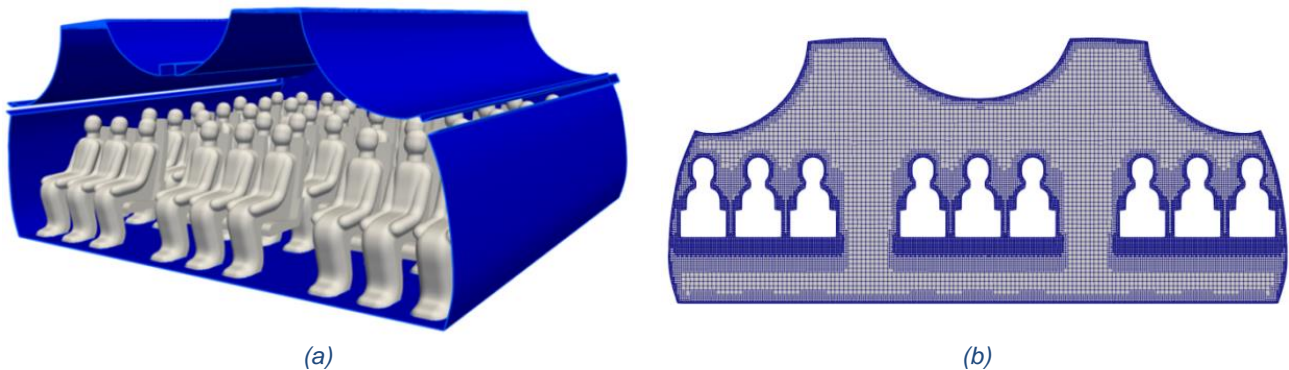


Figure 3: Computational domain and sketch of the mesh.

3.2 Computational Fluid Dynamics Methods

The governing equations are Navier-Stokes equations with Boussinesq approximation:

$$\nabla \cdot \mathbf{u} = 0, \quad (1)$$

$$\frac{\partial \mathbf{u}}{\partial t} + (\mathbf{u} \cdot \nabla) \mathbf{u} = \nu \nabla^2 \mathbf{u} - \frac{1}{\rho_0} \nabla p - \mathbf{g} \beta \theta, \quad (2)$$

$$\frac{\partial \theta}{\partial t} + (\mathbf{u} \cdot \nabla) \theta = \frac{\nu}{Pr} \nabla^2 \theta, \quad (3)$$

where ρ_0 is the reference density, $\theta = T - T_0$ is the deviation of temperature from the reference value T_0 , β is the coefficient of thermal expansion, Pr denotes the Prandtl number and \mathbf{g} represents the

gravity vector. Eqs (1) - (3) describe buoyancy-driven flow provided that the thermal expansion coefficient and temperature variance are small enough:

$$\beta\theta \ll 1. \quad (4)$$

The radiation transfer is computed using the Finite Volume Discrete Ordinates Method (fvDOM) implemented in OpenFOAM to solve the radiation transfer equation (RTE) for a predefined number of directions in the ambient media.

The thermal radiation transfer equation for a gray medium in a general form reads [5]:

$$\frac{\partial I}{\partial s} + (\alpha + \sigma_s)I = \alpha I_b + \frac{\sigma_s}{4\pi} \int_{4\pi} I(s_i)\Phi(s_i, \mathbf{s})d\Omega_i, \quad (5)$$

where $I = I(\mathbf{x}, \mathbf{s})$ is the radiation intensity at position \mathbf{x} along direction \mathbf{s} , $I_b = I_b(\mathbf{x})$ is the black body radiation intensity, $\Phi(s_i, \mathbf{s}) = \Phi(\mathbf{x}, s_i, \mathbf{s})$ is the scattering phase function, $\alpha = \alpha(\mathbf{x})$ and $\sigma_s = \sigma(\mathbf{x}, \mathbf{s})$ are absorption and scattering coefficients, respectively. Since the air is treated as non-participating and non-scattering medium in the simulations, the calculation of Eq. (5) is reduced accordingly.

For the diffusively emitting and reflecting wall boundaries, the following conditions are valid [5]:

$$I(\mathbf{s}) = \varepsilon I_b + \frac{1 - \alpha}{\pi} \int_{(\mathbf{n} \cdot \mathbf{s}') < 0} I(\mathbf{s}') |\mathbf{n} \cdot \mathbf{s}'| d\Omega', \quad (6)$$

where ε is the emissivity coefficient and \mathbf{n} is an outer normal-to-surface vector. The radiative heat flux calculated on the walls,

$$q_r = \int I(\mathbf{s})(\mathbf{n} \cdot \mathbf{s})d\Omega, \quad (7)$$

is further applied as radiative component of the total heat flux in the boundary conditions of Eq. (3). The standard OpenFOAM steady state solver buoyantBoussinesqSimpleFoam is used to solve the system of Eqs. (1) - (3). It is based on the classical SIMPLE algorithm (Semi-Implicit Method for Pressure-Linked Equations), initially developed by Patankar and Spalding [6]. The solver allows for the simulation of a variety of turbulence models, here we use the k- ω -SST turbulence model. Thanks to the fine resolution in the vicinity of the walls, the low Reynolds number approach (Low-Re) is used for near-wall turbulence modeling by applying the following conditions:

- $k = 10^{-16}$ (very small number, not modeled),
- omegaWallFunction for omega (standard ω wall function),
- kinematic turbulent viscosity nut is calculated (not modeled).

Usually, the use of Low-Re conditions leads to an essential improvement of the accuracy of the simulations if they are applied at a well-resolved wall ($y^+ < 5$).

3.3 Comfort Evaluation Measures

In a post-processing tool chain, thermal comfort quantities, such as predicted percentage of dissatisfied (PPD) and predicted mean vote (PMV) are calculated. Thereby, we use for head, body and feet, the clothing insulations of 0.0, 0.6 and 1.0, respectively. This distribution is motivated to represent a more realistic distribution of the typical passenger, wearing no clothes on the head, light clothes on the body and closed shoes at the feet. Further, we used 1.0 as metabolic rate and 0 for the physical activity, corresponding to a sitting passenger at rest.

Predicted Mean Vote

The predicted mean vote (PMV) is a comfort index which reflects the human response to the local thermal environment [7]. It considers both physical environment parameters and individual human

properties:

- air temperature and velocity
- mean radiant temperature
- relative humidity
- metabolic rate
- physical activity
- clothing insulation

The PMV model is based on a series of experiments carried out by P.O. Fanger in the 1970s involving a large group of subjects exposed to a variety of controlled environments. The results of the measurements were evaluated using the 7-point thermal sensation, and then processed statistically with respect to the basic heat balance equation [9].

Predicted Percentage of Dissatisfied

The PPD is an index that establishes a quantitative prediction of the percentage of thermally dissatisfied people who feel too cool or too warm [7]. In Eq. (8) it is related to the PMV index discussed in the previous section:

$$PPD = 100 - 95 \cdot \exp(-0.03353 \cdot PMV^4 - 0.2179 \cdot PMV^2) \quad (8)$$

Draught Rate

Draught is an unwanted local cooling of the body caused by air movements and is considered to be one of the most important local discomfort factors [7]. The comfort index of the draught rate (DR) is defined as the percentage of people predicted to be bothered by draught. The semi-empirical formula

$$DR = (34 - T) \cdot (U - 0.05)^{0.62} \cdot (0.37 \cdot Tu \cdot U + 3.14) \quad (9)$$

was developed by Fanger et al. [10] based on a series of experiments with fifty subjects, dressed to experience a neutral thermal sensation under different conditions of temperature T , mean velocity U and turbulence intensity Tu .

Operative Temperature

The operative temperature T_{op} is defined as the uniform temperature of an imaginary black enclosure in which an occupant would exchange the same amount of heat by radiation and convection as in the actual non-uniform environment [7]. It is defined based on the heat transfer coefficients for radiation and convection as well the air and mean radiant temperatures [8]. Here, the calculation of the operative temperature is conducted on a well-agreed simplified formula [8]:

$$T_{op} \approx \frac{T_{mr} + T \cdot \sqrt{10 \cdot U}}{1 + \sqrt{10 \cdot U}} \quad (10)$$

with the velocity U , the air temperature T and the mean radiant temperature T_{mr} of the surrounding surfaces.

4. Results & Discussion

The effectiveness of the new overhead cooling elements is analysed using computational fluid dynamics simulations in a simplified 5-row, 9-abreast twin-aisle configuration. Herein both cabin displacement ventilation concepts, with and without active cooling elements, are evaluated. For both concepts a mean cabin temperature of 23°C in the passenger zone was realised by supply air temperatures of 21.5 and 22.5°C at a volume flow rate of 16.7 l/s/PAX. The surface temperature of the cooling elements is set to 15°C.

Table 1: Investigated parameter combinations.

Case	V [l/s/PAX]	T _{cabin}	T _{supply}	T _{cooling}
CDV	16.7	23 °C	21.5 °C	---
CDV + RC	16.7	23 °C	22.5 °C	15 °C

Selected results highlighting the effectiveness are presented in Figure 4 to Figure 9 showing the resulting velocity and temperature fields as well as operative temperature, draft rate, PMV and PPD evaluated on the thermal manikins' surface.

4.1 Velocity Distribution

The overall velocity magnitude field of pure cabin displacement ventilation, Figure 4 (a), is highlighted by very low velocities (< 0.1 m/s) in the lower half of the cabin and clearly developed warm thermal plumes around and above the passengers. These are formed by thermal convection and remove the heat from the heated thermal manikins. The comparison of the velocity fields in the central cross section of the computational domain reflects, that there is only a weak impact of the active cooling elements on the velocity field, see Figure 4. Especially in the zone of the seated passenger, no significant differences were found. Further, the overall low velocities, which one of the main advantages of the cabin displacement ventilation, are maintained. Minor differences are found in the upper half of the compartment, where higher velocities above the outer aisle seats (C and G) occur for the case with active cooling compared to pure cabin displacement ventilation.

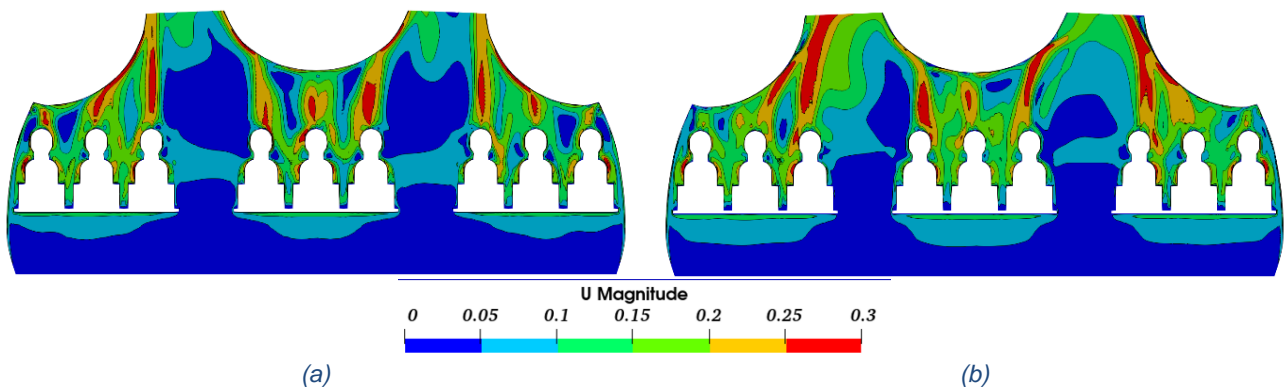


Figure 4: Comparison of velocity distribution at CDV without (a) and with (b) active cooling elements.

4.2 Temperature Distribution

Looking at the temperature data in Figure 5, much lower temperatures can be found in the upper cabin part for the case using active cooling elements, see subfigure (b). The cooling effect clearly reducing the thermal stratification compared to pure cabin displacement ventilation, see subfigure (a). Thereby, the reduction of the colder zone in the lower half of the cabin is a result of the higher temperature of the supply air (22.5 °C vs. 21.5 °C). Despite this increased supply air temperature, the air temperatures in the upper half of the cabin are equal or colder. This effect is caused by two mechanism, firstly, the active cooling elements with 15 °C surface temperature also have a convective part of heat transfer directly reducing the air temperature in the vicinity of the elements. However, this effect is well-balanced in a way, that no cold down-welling plumes establish, see Figure 5 (b). Secondly, the increased radiant heat transfer from the manikins' surface, especially the heads, leads to a reduced convective heat release of the manikins and thus to lower air temperatures in the upper cabin half, visible e.g. as weaker warm thermal plumes above the manikins.

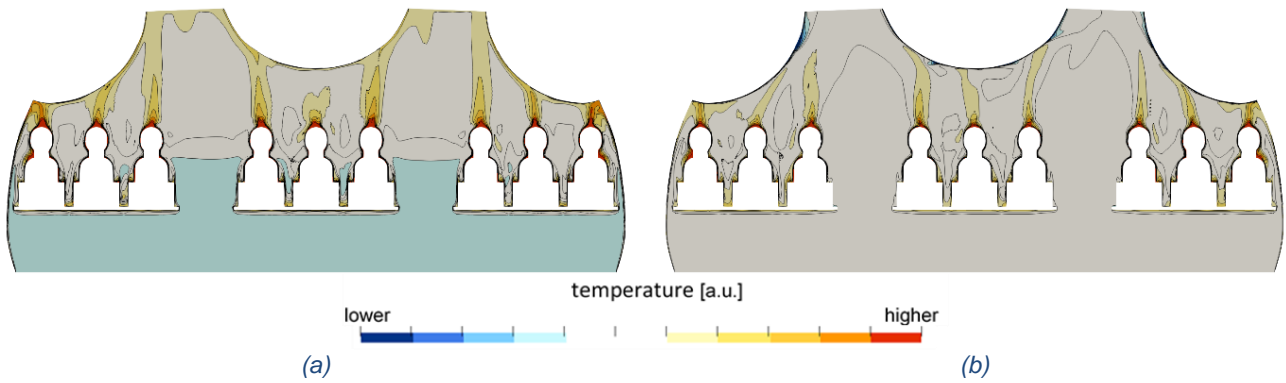


Figure 5: Comparison of temperature distribution at CDV without (a) and with (b) active cooling elements.

4.3 Comfort Parameter

Following the discussion of the velocity and the air temperature fields, we present and discuss selected comfort parameter in this section. These are evaluated in the central row of the computational domain and mapped on the manikins' surfaces. Figure 6 shows the operative temperature, which can be interpreted as a "felt" temperature, due to its definition as a climate sum measure. The typical temperature stratification occurring for pure CDV is visible in (a) and reveals an operative temperature increasing by more than 7 K from feet level to head level. Thereby, a high spatial homogeneity in the cabin confirms another advantage of displacement ventilation. Here, the individual thermal conditions are independent from the seat position. Upon the activation of the cooling elements (b), this homogeneity is slightly reduced and results in small operative temperature differences, especially for the upper body when comparing aisle and non-aisle seats. However, simultaneously the vertical stratification of the operative temperature is also reduced by more than 2 K. As a result, a more comfortable temperature distribution is achieved in the cabin.

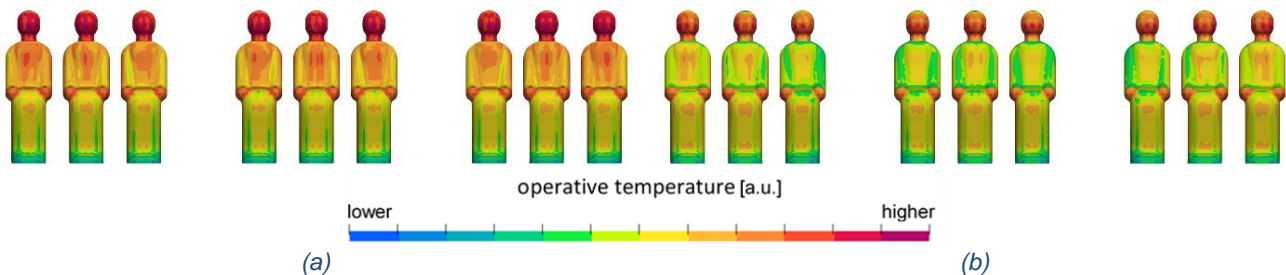


Figure 6: Comparison of operative temperature distribution at CDV without (a) and with (b) active cooling elements.

Additionally, we present the draft rate in Figure 7. For both investigated cases, pure CDV (a) and CDV with active cooling elements (b), low draft rate values are found. These are caused by the low flow velocities in combination with low turbulence intensities and rather high temperatures of the inflowing air, both a direct result of the low-momentum air supply of the cabin displacement ventilation. Consequently, negative effects of the draft rate on the thermal passenger comfort can be neglected for both configurations.

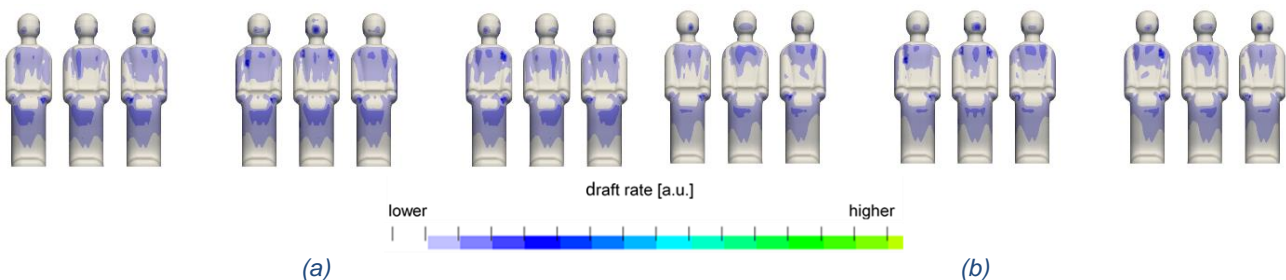


Figure 7: Comparison of draft rate distribution at CDV without (a) and with (b) active cooling elements.

Finally, we present the comfort evaluation in terms of predicted mean vote (PMV) (Figure 8) and the predicted percentage of dissatisfied passenger (PPD) (Figure 9). Thereby, PMV reflects both, too cold (negative values) and too warm (positive values) conditions, whereas PPD estimates the percentage of passengers which might be dissatisfied due to the given thermal conditions. With regard to PMV, it should be noted, that the scale from -3 to +3 can be interpreted as “too cold”, “cold”, “slightly cool”, “neutral”, “slightly warm”, “warm” and “hot”. To achieve comfortable indoor conditions, $|PMV| \leq 0.5$ is desired, whereas $|PMV| \leq 0.8$, corresponding to less than $PPD \leq 20\%$, is often still accepted. The positive effect of the active cooling element already discussed in terms of the operative temperature is confirmed by the PMV evaluation, see Figure 8. For the case with active cooling elements (b), almost all body parts are within the range of $|PMV| \leq 0.5$ and thus rated as comfortable. In contrast, for pure CDV (a) the temperature stratification leads to compromises in comfort characterized by too warm upper body parts.

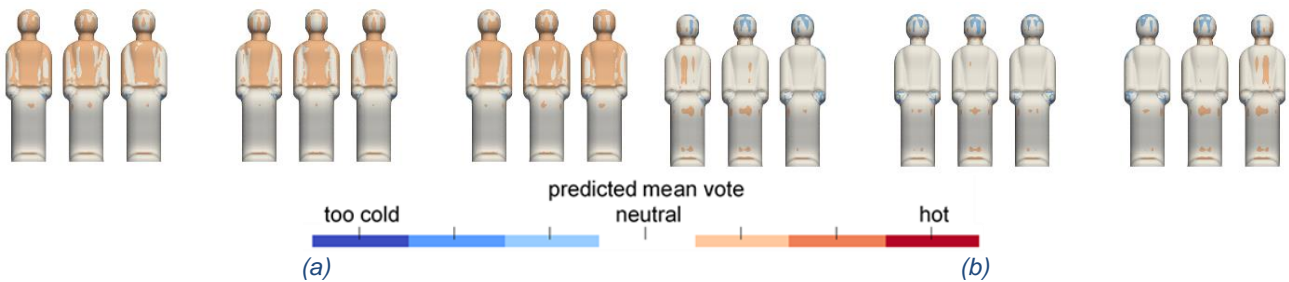


Figure 8: Comparison of predicted mean vote (PMV) distribution at CDV without (a) and with (b) active cooling elements.

The above discussed finding is highlighted by the PPD evaluation, see Figure 9. Herein, we can confirm that the presented overhead cooling devices lead to a significant reduction of the percentage of dissatisfied passengers. Thereby, the spatially resolved evaluation underlines the effectiveness of the overhead cooling devices on the upper body half.

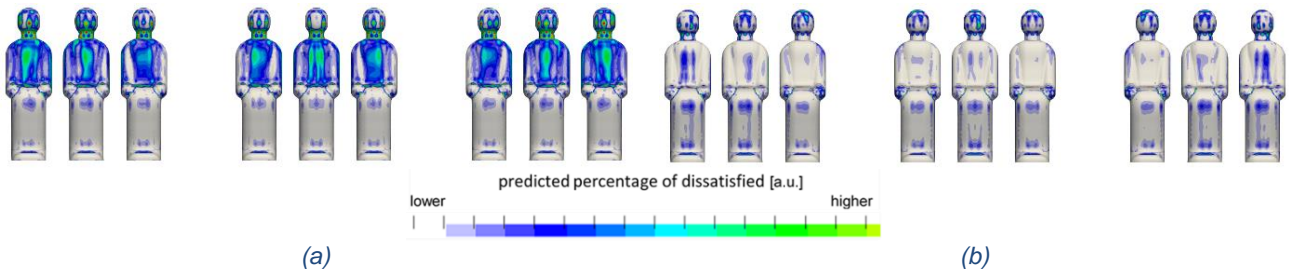


Figure 9: Comparison of predicted percentage of dissatisfied (PPD) distribution at CDV without (a) and with (b) active cooling elements.

5. Conclusion

We presented a new, patent-pending technology brick [4] for an enhanced cooling and ventilation concept for a passenger aircraft cabin. The new device helps to reduce the thermal stratification of displacement ventilation while maintaining the benefits. We discussed the new approach of the “radiant cooling” device with regard to effects on the temperature and velocity distributions as well as on comfort-relevant evaluation parameter such as PMV and PPD within the cabin based on computational fluid dynamics. The results confirmed the positive effects of the overhead cooling devices on the thermal passenger comfort. Thereby, the most beneficial features of cabin displacement ventilation, i.e. low flow velocities, low draft rates and very high spatial homogeneity regarding the conditions on the different seats, are maintained. Simultaneously, the comfort-critical temperature stratification was reduced with regard to the operative “felt” temperature. The PMV evaluation confirmed a much higher thermal comfort. Furthermore, we briefly pointed out possible technical realisation approaches, underlining the capability of integration as stand-alone system or

connected to the airplane ECS.

The experimental validation with a thermally active demonstrator unit will be conducted during the ADVENT project [11] in the modular cabin mock-up (MKG) [12, 13] located at the DLR site in Göttingen.

6. Remark

This project has received funding from the Clean Sky 2 Joint Undertaking under the European Union's Horizon 2020 research and innovation programme under grant agreement No 755596. The responsibility of the content is the authors.

7. Contact Author Email Address

mailto: daniel.schmeling@dlr.de

8. Copyright Statement

The authors confirm that they, and/or their company or organization, hold copyright on all of the original material included in this paper. The authors also confirm that they have obtained permission, from the copyright holder of any third-party material included in this paper, to publish it as part of their paper. The authors confirm that they give permission, or have obtained permission from the copyright holder of this paper, for the publication and distribution of this paper as part of the AEC proceedings or as individual off-prints from the proceedings.

References

- [1] Müller D, Schmidt M & Müller B. Application of a displacement ventilation system for air distribution in aircraft cabins. *Proceedings of the 2011 Aviation System Technology (AST) Workshop*, Hamburg, Germany, 2011.
- [2] Bosbach J, Lange S, Dehne T, Lauenroth G, Hesselbach F & Allzeit M. Alternative ventilation concepts for aircraft cabins. *CEAS Aeronaut J.* 4(3), 301-313, 2013.
- [3] Maier J, Marggraf-Micheel C, Dehne T & Bosbach J. Thermal comfort of different displacement ventilation systems in an aircraft passenger cabin. *Building and Environment.* 111, 256-264, 2017.
- [4] Schmeling D, Dehne T, Lange P, Shishkin A, Dannhauer A, Bosbach J & Gores I. Aircraft cabin and aircraft cabin cooling device. DE102019122963A1, patent pending, 2019.
- [5] Modest M F. *Radiative Heat Transfer*. 3rd ed., Academic, New York, 2013.
- [6] Patankar S & Spalding D. A Calculation Procedure for Heat, Mass and Momentum Transfer in Three-dimensional Parabolic Flows. *Int. J. Heat and Mass Transfer* 15, p. 1787, 1972.
- [7] ISO 7730:2005. Ergonomics of the thermal environment - Analytical determination and interpretation of thermal comfort using calculation of the PMV and PPD indices and local comfort criteria. International Standard Organization, 2005.
- [8] EN ISO 7726:2001. Ergonomics of the thermal environment - Instruments for measuring physical quantities. International Standard Organization, 2001.
- [9] Fanger P. *Thermal Comfort*. Danish Technical Press, Copenhagen, Denmark, 1970.
- [10] Fanger P, Melikov A & Ring J. Air turbulence and sensation of draught. *Energy and Buildings* 12, pp. 21-39, 1988.
- [11] URL: https://www.dlr.de/as/en/desktopdefault.aspx/tabid-17350/27473_read-69992/, online, accessed October, 13th 2021.
- [12] Lange P, Schmeling D, Dehne T, Dannhauer A, Werner W & Gores I. New long-range cabin mock-up enabling the simulation of flight cases by means of tempered fuselage elements. *Proceedings of the 2020 Aerospace Europe Conference*, Bordeaux, France, 2020.
- [13] URL: <https://www.dlr.de/content/en/research-facilities/modular-cabin-mock-up-goettingen-mkg.html>, online, accessed October, 13th 2021.